



# Relativistic complex separable potential for describing the neutron-proton system in ${}^3S_1$ - ${}^3D_1$ partial-wave state

S.G. Bondarenko, V.V. Burov, E.P. Rogochaya

*JINR - Joint Institute for Nuclear Research, Joliot-Curie 6, 141980 Dubna, Moscow region, Russia*

---

## Abstract

Within a covariant Bethe-Salpeter approach the relativistic complex separable kernel of the neutron-proton interaction for the coupled  ${}^3S_1$ - ${}^3D_1$  partial-wave state is constructed. The rank-six separable potential elaborated earlier is real-valued, and therefore makes it possible to describe only the elastic part (phase shifts, low-energy parameters, deuteron properties, etc.) of the elastic neutron-proton scattering. The description of the inelasticity parameter comes out of the imaginary part introduced in the potential. The complex potential parameters are obtained using the available elastic neutron-proton scattering experimental data up to 1.1 GeV.

*Keywords:* elastic neutron-proton scattering, Bethe-Salpeter equation, partial-wave analysis, separable kernel, inelasticity

---

## 1. Introduction

A theoretical description of the neutron-proton ( $np$ ) system makes it possible to understand the nuclear structure. The nucleon-nucleon (NN) scattering is traditionally described in terms of the meson-nucleon theory at low and medium energies. The one-boson exchange (realistic) potential plays a predominant role in this case. At higher energies, production processes and inelasticities become important, and systems composed of nucleons and mesons contribute to the NN scattering. At present there is no quantitative description of the NN scattering above the inelastic threshold neither in terms of QCD nor of meson and nucleon degrees of freedom.

There have been several theoretical attempts built within boson exchange models to explain NN scattering data up to 1 GeV. All of them describe observables perfectly for energies up to 300 MeV. However, using boson exchange potentials at higher energies gives only a qualitative agreement with experimental data. Optical model studies have been suggested for the medium and high energy NN scattering [1, 2]. They give a quantitative agreement with the experimental data for the NN

scattering and Bremsstrahlung within the wide energy range.

The Bethe-Salpeter (BS) approach [3, 4], as a four-dimensional covariant formalism, is the most appropriate to study the NN interaction. It is convenient to use a separable ansatz [4] for the interaction kernel in the BS equation in this picture. Papers [5, 6] have suggested multirank separable potentials to describe the  $np$  scattering with the total angular momentum  $J = 0, 1$  and the deuteron. The obtained potentials can describe all available experimental data for the phase shifts, static properties of the deuteron, and the exclusive electron-deuteron breakup in the plane-wave approximation [5, 6, 7].

However, it is important to investigate the influence of the inelasticity in the elastic NN scattering. We describe the inelasticity using a complex NN potential of a special type [8] instead of the real-valued one obtained earlier in Refs. [5, 6]. The method has been successfully used for the description of the uncoupled partial-wave states of the  $np$  system with the total angular momentum  $J = 0, 1$ . Now we apply it to construct the complex potential for the coupled  ${}^3S_1$ - ${}^3D_1$  partial-wave state.

The paper is organized as follows. In Sec.2, the

parametrization of the scattering matrix is described. The used complex separable interaction kernel is considered in Sec.3. The procedure which we apply to find new imaginary interaction kernel parameters and the obtained parameters are presented in Sec.4. The discussion and conclusion are given in Sec.5.

## 2. Parametrization of the S matrix

Following Arndt et al. [9], we prefer to use the parametrization of the  $K$  matrix rather than the scattering matrix  $S$ :

$$K = i \frac{1 - S}{1 + S} = \text{Re}K + i\text{Im}K, \quad (1)$$

where  $K$  is a  $2 \times 2$  matrix for the coupled partial-wave state. The real part  $\text{Re}K$  is represented as

$$\text{Re}K = i \frac{1 - S_e}{1 + S_e}, \quad (2)$$

where

$$S_e = \begin{pmatrix} \cos 2\varepsilon_1 e^{2i\delta_{<}} & i \sin 2\varepsilon_1 e^{i(\delta_{<} + \delta_{>})} \\ i \sin 2\varepsilon_1 e^{i(\delta_{<} + \delta_{>})} & \cos 2\varepsilon_1 e^{2i\delta_{>}} \end{pmatrix} \quad (3)$$

is the well-known Stapp parametrization [10] for the elastic NN scattering matrix. Here  $\delta_{<} = \delta_{L=J-1}$ ,  $\delta_{>} = \delta_{L=J+1}$  are phase shifts of  ${}^3S_1^+$  and  ${}^3D_1^+$  states, respectively, and  $\varepsilon_1$  is a mixing parameter. The  $\text{Im}K$  is given by

$$\text{Im}K = \begin{pmatrix} \tan^2 \rho_{<} & \tan \rho_{<} \tan \rho_{>} \cos \mu \\ \tan \rho_{<} \tan \rho_{>} \cos \mu & \tan^2 \rho_{>} \end{pmatrix} \quad (4)$$

in terms of the inelasticity parameters  $\rho_{<,>}, \mu$  corresponding to the states with the orbital momenta  $L = J - 1, J + 1$ , and  $\varepsilon_1$  respectively.

## 3. Complex separable kernel

We assume that the interaction kernel  $V$  conserves parity, the total angular momentum  $J$  and its projection, and isotopic spin. Due to the tensor nuclear force, the orbital angular momentum  $L$  is not conserved. The negative-energy two-nucleon states are switched off, what leads to the total spin  $S$  conservation. The partial-wave-decomposed BS equation in the center-of-mass system of the  $np$  pair is therefore reduced to the following form:

$$T_{rl}(p'_0, |\mathbf{p}'|; p_0, |\mathbf{p}|; s) = V_{rl}(p'_0, |\mathbf{p}'|; p_0, |\mathbf{p}|; s) + \frac{i}{4\pi^3} \sum_{l'} \int_{-\infty}^{+\infty} dk_0 \int_0^{\infty} \mathbf{k}^2 d|\mathbf{k}| \times \frac{V_{l'l'}(p'_0, |\mathbf{p}'|; k_0, |\mathbf{k}|; s) T_{rl}(k_0, |\mathbf{k}|; p_0, |\mathbf{p}|; s)}{(\sqrt{s}/2 - E_{\mathbf{k}} + i\epsilon)^2 - k_0^2}. \quad (5)$$

The square of the  $np$  pair total momentum  $s$  is related with the laboratory energy  $T_{\text{Lab}}$  as:  $s = 2mT_{\text{Lab}} + 4m^2$ ,  $m$  is the mass of the nucleon.

To describe the inelasticity in the elastic NN scattering, we modify the real-valued relativistic potential adding the imaginary part:

$$V_r \rightarrow V = V_r + iV_i.$$

To solve the Eq.(5), the separable (rank  $N$ ) ansatz [4] for the NN interaction kernel is used:

$$V_{rl}(p'_0, |\mathbf{p}'|; p_0, |\mathbf{p}|; s) = \sum_{m,n=1}^N \left[ \lambda_{mn}^r(s) + i\lambda_{mn}^i(s) \right] g_i^{[l']}(p'_0, |\mathbf{p}'|) g_j^{[l]}(p_0, |\mathbf{p}|), \quad (6)$$

where the imaginary part  $\lambda^i$  has the following form [8]:

$$\lambda_{mn}^i(s) = \theta(s - s_{th}) \left( 1 - \frac{s_{th}}{s} \right) \bar{\lambda}_{mn}^i, \quad (7)$$

$g_j^{[l]}$  are model functions,  $\lambda_{mn} = \lambda_{mn}^r + i\lambda_{mn}^i$  is a matrix of model parameters and  $s_{th}$  is an inelasticity threshold value (the first energy point where the inelasticity becomes nonzero). In this case, the resulting  $T$  matrix has a similar separable form:

$$T_{rl}(p'_0, |\mathbf{p}'|; p_0, |\mathbf{p}|; s) = \sum_{m,n=1}^N \tau_{mn}(s) g_i^{[l']}(p'_0, |\mathbf{p}'|) g_j^{[l]}(p_0, |\mathbf{p}|), \quad (8)$$

where

$$\left( \tau_{mn}(s) \right)^{-1} = \left( \lambda_{mn}^r(s) + i\lambda_{mn}^i(s) \right)^{-1} + h_{mn}(s), \quad (9)$$

$$h_{mn}(s) = -\frac{i}{4\pi^3} \sum_l \int dk_0 \int \mathbf{k}^2 d|\mathbf{k}| \frac{g_m^{[l]}(k_0, |\mathbf{k}|) g_n^{[l]}(k_0, |\mathbf{k}|)}{(\sqrt{s}/2 - E_{\mathbf{k}} + i\epsilon)^2 - k_0^2}. \quad (10)$$

The functions  $g_m^{[l]}$  and the parameters  $\lambda^r$  coincide with those used in Ref. [6] while  $\lambda^i$  are new parameters which are calculated.

Thus, we introduce the imaginary part  $V_i$  of the potential  $V$  (6) adding the new parameters  $\lambda^i$  to the real part  $V_r$  which is left unchanged. It allows us to describe the additional inelasticity parameters by a minimal change of the previous kernel [6].

#### 4. Calculations and results

The description of the inelastic part in the  ${}^3S_1^+ - {}^3D_1^+$  state is performed in the same way as in our previous paper [8] for the uncoupled partial-wave states. We start from the real-valued rank-six interaction kernel MY6 [6] obtained from the description of low-energy characteristics and phase shifts for the laboratory energies  $T_{\text{Lab}}$  up to 1.1 GeV whose experimental values were taken from the SAID program [11]. The parameters of the real part are fixed. Then  $\lambda^i$  are calculated to give a correct behavior of the inelasticity parameters  $\rho_{<}$ ,  $\rho_{>}$ . The experimental data for them can be taken from the SAID program.

The minimization procedure for the function

$$\chi^2 = \sum_{m=m_{th}}^n \sum_{l=<,>} (\delta_l^{\text{exp}}(s_m) - \delta_l(s_m))^2 / (\Delta\delta_l^{\text{exp}}(s_m))^2 + (\rho_l^{\text{exp}}(s_m) - \rho_l(s_m))^2 / (\Delta\rho_l^{\text{exp}}(s_m))^2 \quad (11)$$

is used. Here  $n$  is the number of available experimental points,  $m_{th}$  is the number of the data point corresponding to the first nonzero  $\rho$  value. It is defined by the threshold kinetic energy  $T_{\text{Lab } th}$  which is taken from the single-energy analysis [11].

The resulting parameters  $\lambda^i$  are listed in Table 1<sup>1</sup>. In Figs.1-3, the results of the phase shift, inelasticity parameter and mixing parameter calculations (MYI6 - red dashed line) are compared with the experimental data, our previous result without inelasticities [6] (MY6 - red solid line; only for the phase shifts and the mixing parameter), the SP07 solution [12] (green dashed-dotted line) and the optical potential FGA [2] (blue dashed-dotted-dotted line).

#### 5. Discussion and conclusion

The obtained phase shifts and inelasticity parameter for the  ${}^3S_1^+$  partial-wave state are presented in Fig.1. We see that all considered calculations (MY6, MYI6, SP07, FGA) give an excellent description of all available experimental data for phase shifts and are quite similar to each other for  $T_{\text{Lab}}$  up to 2 GeV. However, MYI6 model phase shifts suddenly change their behavior at the laboratory energy  $T_{\text{Lab}} \gtrsim 2$  GeV, which becomes similar to FGA (see also SM97, FA00 and SP00 solutions [13]). Therefore, to understand whether this behavior means

<sup>1</sup>We would like to note misprints in Tables 2 and 3 [6] where  $\bar{\lambda}$  (GeV<sup>2</sup>) should be read as  $\bar{\lambda}$  (GeV<sup>4</sup>).

Table 1: Parameters  $\bar{\lambda}^i$  of the rank-six kernel MYI6 for the coupled  ${}^3S_1^+ - {}^3D_1^+$  state.

$\bar{\lambda}_{11}^i$ (GeV <sup>2</sup> )	-366.6091
$\bar{\lambda}_{12}^i$ (GeV <sup>2</sup> )	128.6970
$\bar{\lambda}_{13}^i$ (GeV <sup>2</sup> )	-0.3089566
$\bar{\lambda}_{14}^i$ (GeV <sup>2</sup> )	-68.07828
$\bar{\lambda}_{15}^i$ (GeV <sup>2</sup> )	64.67047
$\bar{\lambda}_{16}^i$ (GeV <sup>2</sup> )	-11.51058
$\bar{\lambda}_{22}^i$ (GeV <sup>2</sup> )	68.53852
$\bar{\lambda}_{23}^i$ (GeV <sup>2</sup> )	3.129745
$\bar{\lambda}_{24}^i$ (GeV <sup>2</sup> )	458.8815
$\bar{\lambda}_{25}^i$ (GeV <sup>2</sup> )	2669.315
$\bar{\lambda}_{26}^i$ (GeV <sup>2</sup> )	11.35009
$\bar{\lambda}_{33}^i$ (GeV <sup>2</sup> )	-2.395499
$\bar{\lambda}_{34}^i$ (GeV <sup>2</sup> )	15.130951
$\bar{\lambda}_{35}^i$ (GeV <sup>2</sup> )	-55.78875
$\bar{\lambda}_{36}^i$ (GeV <sup>2</sup> )	0.4364534
$\bar{\lambda}_{44}^i$ (GeV <sup>2</sup> )	411.3334
$\bar{\lambda}_{45}^i$ (GeV <sup>2</sup> )	3280.671
$\bar{\lambda}_{46}^i$ (GeV <sup>2</sup> )	-11.29448
$\bar{\lambda}_{55}^i$ (GeV <sup>2</sup> )	5685.375
$\bar{\lambda}_{56}^i$ (GeV <sup>2</sup> )	-44.92390
$\bar{\lambda}_{66}^i$ (GeV <sup>2</sup> )	-0.07438475
$T_{\text{Lab } th}$ (GeV)	0.4

some physical effect or the model needs to be improved, the experimental data at  $T_{\text{Lab}} > 1.1$  GeV are necessary. The description of the inelasticity parameter is perfect for the MYI6, FGA potentials and the SP07 solution for  $T_{\text{Lab}}$  up to 1.1 GeV where the experimental data are available and they are different at higher energies.

Fig.2 shows the results of the calculations for the  ${}^3D_1^+$  state. All of model calculations (MY6, MYI6, SP07, FGA) are in a good agreement with the experimental data and different at the laboratory energies  $T_{\text{Lab}} \gtrsim 1.1$  GeV.

The mixing parameter  $\varepsilon_1$  is depicted in Fig.3. As it is seen from the figure, the MY6 model does not describe it at all. The MYI6 model has similar behavior as MY6 and differ from it at the kinetic energies  $T_{\text{Lab}} \gtrsim 1.1$  GeV.

It is seen that the proposed MYI6 potential gives a consistent description of the existing experimental data for the phase shifts and the inelasticity parameter in the coupled  ${}^3S_1^+ - {}^3D_1^+$  partial-wave state. It should be noted that since all parameters of the real-valued separable interaction kernel ( $\lambda'$ ,  $\beta$  and  $\alpha$ ) found in the previous analysis [6] have been fixed, the MY6 and MYI6 model phase shifts coincide up to  $T_{\text{Lab}} < T_{\text{Lab } th}$  and are different at  $T_{\text{Lab}} > T_{\text{Lab } th}$ . The comparison of four different calculations MY6, MYI6, SP07, FGA has shown that

the experimental data for the phase shifts and inelasticity parameter at higher laboratory energies are vitally necessary to define the behavior of the NN potential precisely.

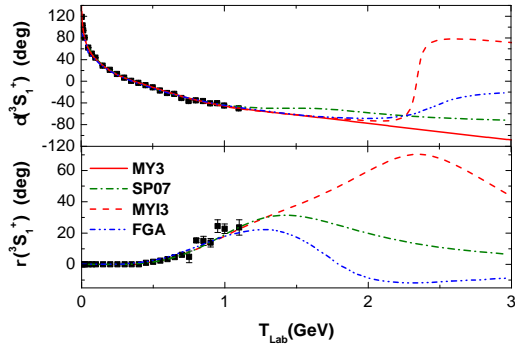


Figure 1: Phase shifts and inelasticity parameter for the  ${}^3S_1^+$  partial-wave state. The results of calculations with the potentials - real-valued MY6 [6], complex MY16, optical FGA [2] and the SP07 solution [12] are compared.

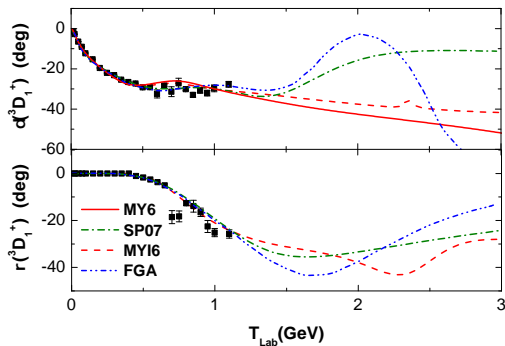


Figure 2: Phase shifts and inelasticity parameter for the  ${}^3D_1^+$  partial-wave state. The notations are the same as in Fig.1.

## 6. Acknowledgments

We would like to thank the organizers of the 5th Joint International HADRON STRUCTURE'11 Conference (June 27th - July 1st, 2011, Tatranská Štrba, Slovak Republic) for invitation, support and opportunity to present our new results.

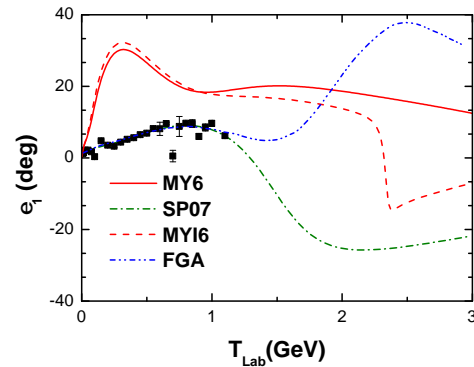


Figure 3: Mixing parameter  $\epsilon_1$ . The notations are the same as in Fig.1.

## References

- [1] V.A. Knyr, V.G. Neudachin, N.A. Khokhlov, Phys. Atom. Nucl. 69 (2006) 2034; N.A. Khokhlov, V.A. Knyr, Phys. Rev. C 73 (2006) 024004.
- [2] A. Funk, H.V. von Geramb, K.A. Amos, Phys. Rev. C 64 (2001) 054003, arXiv:nucl-th/0105011.
- [3] E.E. Salpeter, H.A. Bethe, Phys. Rev. 84 (1951) 1232.
- [4] S.G. Bondarenko *et al.*, Prog. Part. Nucl. Phys. 48 (2002) 449, arXiv:nucl-th/0203069.
- [5] S.G. Bondarenko *et al.*, Nucl. Phys. A 832 (2010) 233, arXiv:0810.4470 [nucl-th].
- [6] S.G. Bondarenko *et al.*, Nucl. Phys. A 848 (2010) 75, arXiv:1002.0487 [nucl-th].
- [7] S.G. Bondarenko, V.V. Burov, E.P. Rogochaya, Few Body Syst. 49 (2010) 121, arXiv:1008.0107 [nucl-th].
- [8] S.G. Bondarenko, V.V. Burov, E.P. Rogochaya, arXiv:1106.4478 [nucl-th].
- [9] R.A. Arndt, L.D. Roper, Phys. Rev. D 25 (1982) 2011; R.A. Arndt *et al.*, Phys. Rev. D 28 (1983) 97.
- [10] H.P. Stapp, T.J. Ypsilantis, N. Metropolis, Phys. Rev. 105 (1957) 302-310.
- [11] <http://gwdac.phys.gwu.edu>
- [12] R.A. Arndt *et al.*, Phys. Rev. C 76 (2007) 025209, arXiv:0706.2195 [nucl-th].
- [13] R.A. Arndt *et al.*, Phys. Rev. C 56 (1997) 3005, arXiv:nucl-th/9706003; R.A. Arndt, I.I. Strakovsky, R.L. Workman, Phys. Rev. C 62 (2000) 034005, arXiv:nucl-th/0004039.



Available online at [www.sciencedirect.com](http://www.sciencedirect.com)



Nuclear Physics B Proceedings Supplement 00 (2021) 1–1

---

---

**Nuclear Physics B  
Proceedings  
Supplement**

---

---

---

**Abstract**

*Keywords:*

---

**1.**

arXiv:1108.4170v1 [nucl-th] 21 Aug 2011